BIOCHEMISTRY
including biophysical chemistry & molecular biology
Article

Biochemistry **2010,** *49,* 4235–4243 4235
DOI: 10.1021/bi9020956

Regions and Residues of an Asymmetric Operator DNA Interacting with the Monomeric Repressor of Temperate Mycobacteriophage L1†

Amitava Bandhu,‡,∥ Tridib Ganguly,§,∥ Biswanath Jana,‡ Rajkrishna Mondal,‡ and Subrata Sau*,‡

‡*Department of Biochemistry, Bose Institute, P1/12-CIT Scheme VII M, Kolkata, WB 700 054, India, and* §*Department of Biological Sciences, IISER, Kolkata, WB, India.* ∥*These authors contributed equally to this work.*

Received December 7, 2009; Revised Manuscript Received March 28, 2010

ABSTRACT: Previously, the repressor protein of mycobacteriophage L1 bound to two operator DNAs with dissimilar affinity. Surprisingly, the putative operator consensus sequence, 5′GGTGGa/cTGTCAAG, lacks the dyad symmetry reported for the repressor binding operators of λ and related phages. To gain insight into the structure of the L1 repressor−asymmetric operator DNA complex, we have performed various in vitro experiments. A dimethyl sulfate protection assay revealed that five guanine bases, mostly distributed in the two adjacent major grooves of the 13 bp operator DNA helix, participate in repressor binding. Hydroxyl radical footprinting demonstrated that interaction between the repressor and operator DNA is asymmetric in nature and occurs primarily through one face of the DNA helix. Genetic studies not only confirmed the results of the dimethyl sulfate protection assay but also indicated that other bases in the 13 bp operator DNA are critical for repressor binding. Interestingly, repressor that weakly induced bending in the asymmetric operator DNA interacted with this operator as a monomer. The tertiary structure of the L1 repressor−operator DNA complex therefore appears to be distinct from those of the lambdoid phages even though the number of repressor molecules per operator site closely matched that of the λ phage system.

The key regulatory elements that most temperate bacteriophages employ for the establishment and maintenance of lysogeny are the phage-encoded repressor and the cognate operator DNA (*1*−*10*). To ensure phage lysogeny, repressor protein generally inhibits the transcription of the phage-specific lytic genes from the early promoter by binding to the overlapping operator DNA. The molecular mass and the primary structure of the phage-specific repressor proteins vary greatly, but they typically harbor a DNA binding domain and a separate oligomerization domain. The operator DNAs, which may be symmetric (*1*−*6*) or asymmetric in nature (*7*−*10*), differ in size and in sequence. Investigation of the structures of several phage-specific repressor−operator complexes demonstrated that the operator binding forms of repressors are typically multimeric in nature (*2*, *11*−*13*), with numerous residues from both repressor and operator DNA contributing to complex development. The architectures of most complexes, especially, which are formed between the repressors and cognate asymmetric operator DNAs, have not been well-characterized.

Mycobacteriophage L1,[1] a temperate bacteriophage, utilizes *Mycobacterium smegmatis* as the host for executing its lytic and lysogenic life cycles (*14*). Genetic analysis has revealed that L1 harbors 28 genes for regulating lytic development and a repressor (*cI*) gene for maintaining lysogeny (*15*). The *cI* gene was cloned, sequenced, and found to encode a protein of 183 amino acid residues (*16*). Both the native L1 repressor (CI) and its N-terminal histidine-tagged variant (His-CI) were purified to homogeneity and exploited in investigating the structure and DNA binding capacity of this regulatory protein at length (*10*). CI monomer appears to possess an N-terminal domain (NTD), a C-terminal domain (CTD), and a small hinge region between the two domains. The NTD, which consists of amino acid residues ∼1−54, carries a putative helix−turn−helix (HTH) motif, indicating its possible role in operator DNA binding. Indeed, a variant L1 repressor lacking HTH motif did not bind to the cognate operator DNA at a detectable level (*17*). The CTD, which is composed of amino acid residues ∼63−183, exhibited more compactness than the NTD and appeared as a dimer in solution, suggesting the involvement of this domain in CI dimerization (*10*). The α-helical contents of both CI and CTD were reduced substantially when their incubation temperature was increased from 30 to 42 °C, demonstrating that these proteins unfold at higher temperatures. Expectedly, operator DNA binding activity of CI at 42 °C was found to be less than that at 30 °C (*18*). Other physical factors that strongly influence the structure and function of CI are the ions and the ionic strength of the solution (*17*, *19*). Na^+ turns out to be a better ion than other monovalent cations and Mg^{2+} for maintaining the structure, function, and stability of CI.

Previously, CI bound to two different L1 DNA fragments (designated O_{64} and O_L) with dissimilar affinity (*10*). While O_{64} carries the putative operator sequence 5′GGTGGATGTCAAG, O_L harbors the sequence 5′GGTGGCTGTCAAG. The

†The work was supported by grants from CSIR, Government of India [37(1194)/04/EMR-II], and BRNS/DAE, Government of India (2007/37/26/BRNS/1907), to S.S. A.B. received a senior research fellowship from CSIR (Government of India).

*To whom correspondence should be addressed: Department of Biochemistry, Bose Institute, P1/12-CIT Scheme VII M, Kolkata, WB 700 054, India. E-mail: subratasau@gmail.com or sau@bic.boseinst.ernet.in. Phone: 91-33-2569-3200. Fax: 91-33-2355-3886.

[1]Abbreviations: L1, mycobacteriophage L1; L5, mycobacteriophage L5; CI, native L1 repressor; His-CI, N-terminal histidine-tagged L1 CI; MBP-CI, N-terminal maltose binding protein-tagged L1 CI; NTD, N-terminal domain of L1 CI; CTD, C-terminal domain of L1 repressor; DMS, dimethyl sulfate.

Published on Web 04/08/2010

apparently higher repressor binding affinity observed with the former operator might be due to the "A" base at the sixth position which is a "C" in the latter sequence. Surprisingly, unlike the repressor binding operator DNAs of the lambdoid phages (*2*), putative L1 operators are asymmetric in nature. Repressor proteins of mycobacteriophages L5 and Bxb1 also exhibited binding to asymmetric operator DNAs (*9*, *20*). Interestingly, both L5 and Bxb1 carry multiple asymmetric operator sites, which are dispersed at various genome locations (*9*). Sequences of CI and its cognate operator DNAs show 100% identity with those of L5 and moderate identity with those of Bxb1 (*16*, *21*). Currently, little is known about the nucleotides, grooves, or faces of the asymmetric operator DNA involved in the binding of any mycobacteriophage-specific repressor protein. The tertiary structure of any asymmetric operator DNA−repressor complex has also not yet been determined. Using the repressor−O_{64} operator system of mycobacteriophage L1 as a model system, here we studied the interactions between these two regulatory elements by several in vitro techniques. Our data confirm that the 13 bp asymmetric operator DNA indeed participates in repressor binding. Bases that showed interaction with repressor are mostly distributed in the two adjacent major grooves of the operator DNA helix, and the repressor interacts with one face of the asymmetric operator DNA helix. Furthermore, L1 repressor that bends the operator DNA weakly binds to this operator as a monomer even though its concentration in lysogens was found to be reasonably high.

Table 1: Oligonucleotides Used in This Study

oligo	sequence (5′−3′)
64F	GAGAGATCTTAGTGCAGATCAACGACTTCG
64R	ACTAAGCTTGCCGATCCGGCGATGAG
WT1	TTTGGTGGATGTCAAGTTAGA
WT2	CTAACTTGACATCCACCAAAA
MIF	TTTGTGGATGTCAAGTTAGA
MIR	CTAACTTGACATCCACAAAA
M2F	TTTGTTGGATGTCAAGTTAGA
M2R	CTAACTTGACATCCAACAAAA
M3F	TTTGGTCGATGTCAAGTTAGA
M3R	CTAACTTGACATCGACCAAAA
M4F	TTTGGTGGAGGTCAAGTTAGA
M4R	CTAACTTGACCTCCACCAAAA
M5F	TTTGGTGGATTTCAAGTTAGA
M5R	CTAACTTGAAATCCACCAAAA
M6F	TTTGGTGGATGCCAAGTTAGA
M6R	CTAACTTGGCATCCACCAAAA
M7F	TTTGGTGGATGTCTAGTTAGA
M7R	CTAACTAGACATCCACCAAAA
M8F	TTTGGTGGATGTCAACTTAGA
M8R	CTAAGTTGACATCCACCAAAA
B1	ACTTCGGTCACTAACTTGACATC
B1′	GCGTCGGAGGTACACGC
B2	GAATTCGAGCTCGGTACCC
B2′	GCGATGAGTGCGGTGGC
B3	GGAAACAGCTATGACCATGATTAC
B3′	TTCTTCATGTTCGCTACTTTCTG
B4	GAGCGGATAACAATTTCACACAG
B4′	GTTTGGTGGATGTCAAGTTAGTG

EXPERIMENTAL PROCEDURES

Materials. All chemicals, including acrylamide, bisacrylamide, agarose, urea, dimethyl sulfate (DMS), ferrous ammonium sulfate, thiourea, and hydrogen peroxide (H_2O_2), were purchased from Sigma and Merck. The Ni-NTA resin and anti-His antibody were procured from Qiagen. The alkaline phosphatase-tagged goat anti-mouse antibody (IgG1-AP) was procured from Santa Cruz Biotechnology Inc. Radioactive nucleotides, [γ-^{32}P]ATP and [α-^{32}P]dATP, were bought from BARC (Mumbai, India). Restriction and modifying enzymes, Proofstart DNA polymerase, the plasmid isolation kit, the QIAquick gel extraction kit, the QIAquick nucleotide removal kit, the plasmid isolation kit, the PCR kit, oligonucleotides (Table 1), protein, and DNA markers were obtained from Qiagen, Hysel India Pvt Ltd., Genetix Biotech Asia Pvt Ltd., and Roche. Growth media were purchased from Difco Laboratories and HiMedia. Polyclonal anti-CI antibody, raised by injecting His-CI into a rabbit, was bought from Imgenex Biotech Pvt. Ltd.

Bacterial and Phage Strains. *M. smegmatis* strains mc^{2}155 and mc^{2}155 (L1) (i.e., mc^{2}155 with the chromosomally integrated L1 genomic DNA or L1 lysogen) were grown in Middlebrook 7H9 broth (*10*, *15*). *Escherichia coli* strains were routinely cultivated in Luria-Bertani medium supplemented with an appropriate antibiotic (*22*). Mycobacteriophage L1 and its growth conditions were described previously (*15*).

Basic DNA and Protein Techniques. Plasmid DNA isolation, DNA estimation, digestion of DNA by restriction enzymes, modification of DNA fragments by modifying enzymes, plasmid DNA transformation of *E. coli* or *M. smegmatis*, polymerase chain reaction (PCR), purification of DNA fragments, labeling of DNA fragments with either [γ-^{32}P]ATP or [α-^{32}P]dATP, agarose gel electrophoresis, native PAGE, SDS−PAGE, urea-PAGE, staining of polyacrylamide gels, etc., were performed by standard procedures (*9*, *10*, *22*, *23*) or according to the protocols provided by the respective manufacturers (Qiagen, Fermentas GmbH, Bangalore Genei P. Ltd.). The total protein content was estimated by the Bradford assay using bovine serum albumin as the standard (*24*). Isolation of L1 chromosomal DNA was conducted via a previously described procedure (*15*).

Plasmid Construction. To generate different O_{64} operator-carrying DNA fragments, plasmid p1223 was constructed by cloning a 239 bp *Bgl*II−*Xho*I DNA fragment of p1095 (*25*) into the *Bam*HI- and *Sal*I-digested pUC18 vector (*22*). To overexpress the L1 repressor as an N-terminal maltose binding protein (MBP)-tagged variant (MBP-CI), plasmid p1047 was generated via insertion of an L1 DNA fragment [amplified from L1 chromosomal DNA by primers LCP2 and LCP3 (*10*)] into pMAL-C2 (New England Biolab). Construction of plasmid pSAU1180, used for overexpressing His-CI, was reported previously (*10*).

Purification of Recombinant L1 Repressors. To study the CI−operator interaction in detail, we purified His-CI from induced *E. coli* BL21 (DE3) (pSAU1180) cells by Ni-NTA affinity chromatography using the method of Ganguly et al. (*10*). Because of simpler purification procedures and the sufficiently high operator binding activity (*19*), His-CI was preferred over CI and was used in most of the in vitro experiments described here.

To study the CI binding stoichiometry, MBP-CI was purified from *E. coli* ER2523 (p1047) cells according to a standard procedure (*23*) with modifications. Briefly, a log phase *E. coli* ER2523 (p1047) cell culture was induced with 0.1 mM IPTG (isopropyl β-D-1-thiogalactopyranoside) for 4 h at 25 °C. Cells were harvested by centrifugation, washed once with 0.9% NaCl, and resuspended in $^1/_{20}$ volume of buffer A [50 mM sodium phosphate buffer (pH 7.0), 200 mM NaCl, 1 mM EDTA, and 5% glycerol] containing 100 μg/mL PMSF. After the cells had been

ruptured by sonication, cell debris was removed from the crude extract by centrifugation. The resulting cell supernatant was subjected to amylose resin-based affinity chromatography followed by the elution of the protein as described previously (*23*). From SDS−10% PAGE analysis (data not shown), the elution fraction described above was found to possess primarily a protein of ~65 kDa (~95% pure). The molecular mass of this eluted protein corresponded to the calculated molecular mass of MBP-CI. The purified protein interacted with the anti-CI antibody (data not shown) and exhibited specific binding with O_{64} DNA (Figure S1A of the Supporting Information). The data together indicate that the ~65 kDa protein in the elution fraction was indeed MBP-CI. Both MBP-CI and His-CI were dialyzed against buffer A for 3 h at 4 °C before in vitro experiments were performed. Using the molecular masses of monomeric MBP-CI and His-CI, their respective molar concentrations were determined.

Synthesis of DNA Fragments for in Vitro Studies. To study the structure of the L1 CI−O_{64} DNA complex precisely, several O_{64} operator-carrying DNA fragments were generated by standard procedures (*22*). Briefly, B1, B2, B3, B4, and O_{64} DNA fragments (each 119 bp) were amplified from p1223 DNA by the primer pairs B1 and B1′, B2 and B2′, B3 and B3′, B4 and B4′, and 64F and 64R, respectively (Table 1). All the DNA fragments described above harbor the 13 bp O_{64} operator sequence at different locations. Several other DNA fragments such as M1−M8 and WT were generated by standard annealing of the primer pairs M1F and M1R, M2F and M2R, M3F and M3R, M4F and M4R, M5F and M5R, M6F and M6R, M7F and M7R, M8F and M8R, and WT1 and WT2, respectively (Table 1). All the DNA fragments mentioned above except WT harbor a mutated O_{64} sequence.

Mutant Operator DNA−CI Interaction. To determine the effects of different operator DNA mutations on CI binding, gel shift assays were performed by a standard procedure (*10*) with minor modifications. Briefly, different ^{32}P-labeled mutant operator DNAs (such as M1−M8) were incubated separately with a saturating amount of His-CI in 20 μL of buffer A for 20 min at 25 °C. After termination of the reactions with the gel loading dye (without SDS), all reaction mixtures were analyzed by 6% native PAGE. Binding of His-CI to WT DNA (harboring the 13 bp wild-type operator) was also conducted simultaneously for the sake of comparison.

Chemical Cross-Linking. To determine the oligomeric status of L1 repressor in the presence or absence of cognate operator DNA, we performed chemical cross-linking experiments according to the standard procedure with modifications (*10*). Briefly, different pre-equilibrated reaction mixtures containing 16 μM His-CI and 0−500 nM O_{64} DNA were exposed to a 0.1% glutaraldehyde solution for 2 min at room temperature. We terminated the reactions by adding gel loading dye and boiling the sample for 2 min. All samples were analyzed by 10% SDS−PAGE (*22*).

Gel Shift Assay. To determine the operator binding affinity of MBP-CI, equilibrium binding of this recombinant repressor was studied by a gel shift assay according to the standard procedures (*10*, *18*) with minor modifications. Briefly, varying amounts of MBP-CI were incubated with ~0.2 nM ^{32}P-labeled O_{64} DNA for 20 min at 25 °C followed by the addition of gel loading dye (without SDS) to all reaction mixtures, which were subsequently analyzed by 6% native PAGE (*22*). The autoradiogram (Figures S1B of the Supporting Information) was scanned with a densitometer (Bio-Rad), and the resulting data were used in estimating the amounts of operator DNA bound by MBP-CI. The apparent equilibrium dissociation constant or K_d (i.e., the concentration of MBP-CI yielding half-maximal binding) was determined by nonlinear fitting of the gel shift assay data (described above) to a hyperbola equation using GraphPad Prism.

For studying CI binding stoichiometry, gel shift assays were performed essentially by the same method described above except that reaction mixtures contained 0.2−4 μM His-CI and excess O_{64} DNA (3 μM cold and ~0.2 nM ^{32}P-labeled O_{64} DNA). The His-CI preparation used in the binding stoichiometry experiment was considered to possess 100% operator binding activity.

Mixed Oligomerization Assay. To determine the operator DNA binding form of CI directly, we conducted a mixed oligomerization assay according to the standard procedure with modifications (*26*). In brief, MBP-CI, His-CI, and the pre-equilibrated mixtures of MBP-CI and His-CI were incubated separately with ~0.2 nM ^{32}P-labeled O_{64} DNA for 20 min at room temperature. All reaction mixtures were next analyzed by the procedure as described for the gel shift assay described above.

Bending Study. To study the possible CI-induced bending of the operator DNA, a gel shift assay was performed by the standard procedure (*10*) with minor modifications. Briefly, five ^{32}P-labeled DNA fragments (B1−B4 and O_{64}) were incubated separately with 0.4 μM His-CI followed by the resolution of all reaction mixtures by 8% native PAGE for 8−10 h at 4 °C. The distances between the centers of migrated bands and the origin were determined. The migration of each His-CI−DNA complex was normalized by dividing the migration of the corresponding free DNA. The bending angle α was calculated with the following equation (*27*):

$$\mu_{max}/\mu_{min} = \cos(\alpha/2) \quad (1)$$

μ_{max} and μ_{min} denote the maximally and minimally retarded migrations of the His-CI−DNA complexes, respectively. The apparent bending center was determined from the plot of mobility versus the distance of the O_{64} operator from the 5′ end of the DNA.

Labeling of the Top and Bottom Strands of O_{64} DNA. To label the top strand of O_{64} DNA with ^{32}P, the 5′ end of 64F oligo was labeled with [γ-^{32}P]ATP followed by PCR amplification of 119 bp O_{64} DNA using labeled 64F and 64R and p1223 DNA as the template. Finally, the top strand labeled O_{64} DNA was purified from an agarose gel using the QIAquick gel extraction kit (Qiagen). To label the bottom strand of O_{64} DNA with ^{32}P, the oligonucleotide 64R was end labeled with [γ-^{32}P]ATP followed by the PCR amplification of O_{64} DNA by Taq polymerase using p1223 DNA as the template and the oligonucleotides 64F and labeled 64R as primers. The resulting DNA fragment was purified from an agarose gel by the same method as stated above.

DMS Protection Assay. To identify which guanine bases of the operator DNA interact with CI, a DMS protection assay was performed following Ramesh and Nagraja (*26*) with modification. Briefly, ~0.5 μM His-CI was incubated with 60 nM ^{32}P-labeled O_{64} DNA (~5000 cpm) in 100 μL of phosphate buffer for 20 min at room temperature followed by the treatment of the repressor−operator complexes with 0.2% DMS for 2 min at room temperature. After termination of the reaction with DMS stop solution [1.5 M sodium acetate (pH 7.0) and 1 M β-mercaptoethanol], DNA fragments were recovered by extraction of the reaction mixture with the phenol/chloroform mixture

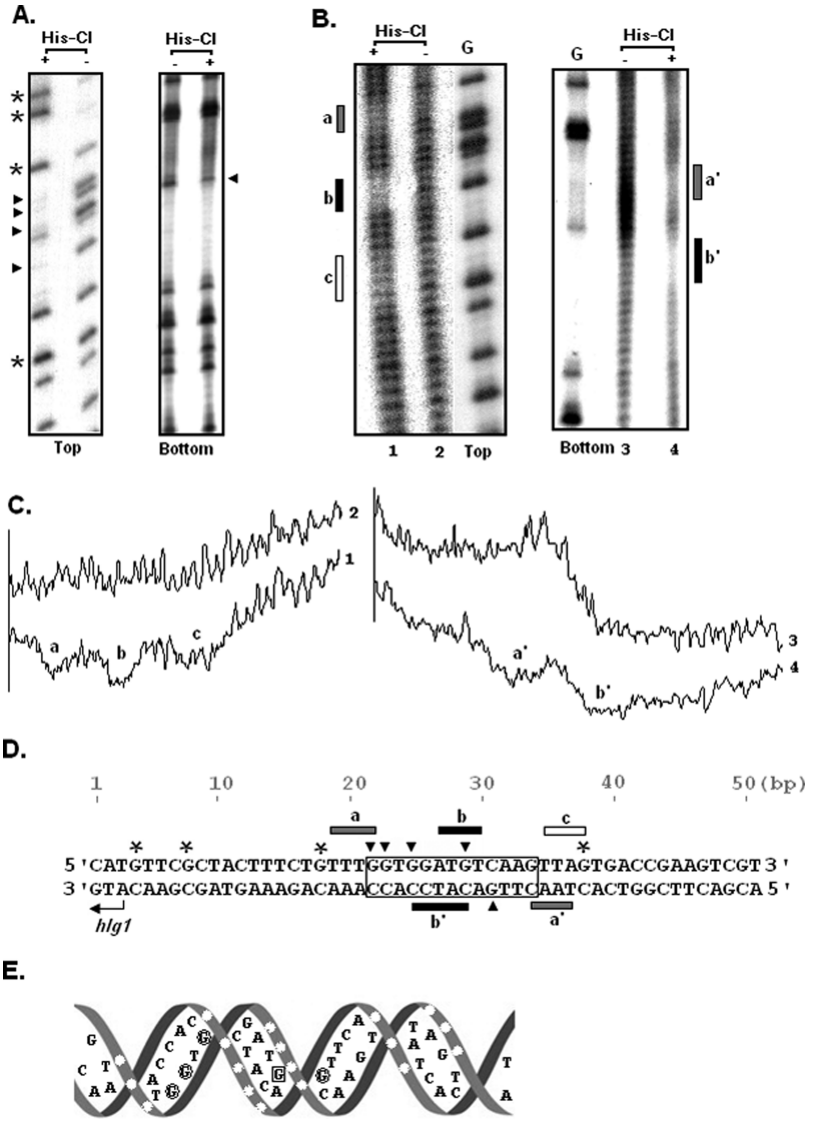

FIGURE 1: Analysis of different DNA footprints. Unless otherwise stated, all footprinting experiments were performed three or four times and only representative data are presented here. (A) Autoradiograms of DMS protection footprints. O_{64} DNA, labeled on the top (Top) or bottom (Bottom) strand, was incubated with (+) or without (−) a saturating amount of CI followed by treatment of the reaction mixture with DMS as described in Experimental Procedures. Asterisks and arrowheads indicate the hypermethylation sites and protected guanine bases, respectively. (B) Autoradiograms of the hydroxyl radical footprints. Hydroxyl radical footprinting was performed according to the procedure described in Experimental Procedures using O_{64} DNA, labeled on the top (Top) or bottom (Bottom) strand in the presence (+) or absence (−) of His-CI. The guanine (G) markers were generated from the top or bottom strand labeled O_{64} DNA by the method of Maxam and Gilbert (*28*). Black (b and b′), gray (a and a′), and white (c) bars indicate the strongest, intermediate, and weakest protected regions, respectively. (C) Densitometric traces of the hydroxyl radical footprints. Traces 1−4 were generated by scanning lanes 1−4 from the top to bottom of the autoradigraphs in panel B. a, a′, b, b′, and c bear the same meaning as in panel B. (D) Summary of the footprinting experiments. The DNA sequence shows the 13 bp O_{64} operator region (boxed) at the upstream of L1 *hlg1* (*25*). The bars (a, b, c, a′, and b′) on the top and bottom of the sequence indicate the hydroxyl radical-protected regions. The color of each bar has the same meaning as in panel B. The protected guanine and hypermethylated bases detected in the DMS footprinting are indicated as shown in panel A. The 50 bp DNA sequence was numbered from left to right. (E) Projection of the footprinting data on the B-DNA helix of O_{64} DNA. The "G" bases that interact with His-CI are encircled or squared, whereas the hydroxyl radical-protected regions on the perimeter are indicated by colorless spots. See the text for details.

(1:1) followed by ethanol precipitation in the presence of glycogen. The same labeled O_{64} DNA was also treated directly with DMS as described above, in the absence of His-CI, and the recovered DNA was used as a control. Finally, both experimental and control DNA fragments were analyzed by urea-8% PAGE .

Hydroxyl Radical Footprinting. To detect which regions of the operator DNA make contacts with CI, the hydroxyl radical footprinting assay was performed using the method of Ramesh and Nagaraja (*26*) with minor modifications. Briefly, 0.5 μM His-CI was incubated with 60 nM ^{32}P-labeled O_{64} DNA (~5000 cpm) in 88 μL of phosphate buffer for 20 min at room temperature followed by the treatment of repressor−operator complexes with 4 μL each of 125 mM Fe(II) ammonium sulfate/250 mM EDTA, 28 mM sodium ascorbate, and 0.84% H_2O_2. The reaction was stopped after 2 min by addition of 10 μL of 100 mM thiourea. The cleaved DNA fragments were purified and analyzed by urea-8% PAGE along with a G-specific ladder, generated from the identical labeled DNA fragments by the standard procedure (*28*).

L1 Repressor Concentration in Lysogens. To determine the CI concentration in lysogens, cells harvested from 300 mL of exponentially growing *M. smegmatis* mc^{2}155 (L1) culture (OD_{590} = 0.4) were resuspened in 8 mL of lysis buffer [50 mM

sodium phosphate buffer (pH 7.0), 200 mM NaCl, 1 mM EDTA, 5% glycerol, and 100 μg/mL PMSF] followed by the preparation of the crude extract by appropriate sonication. After clarification of the crude extract by centrifugation, ~7.4 mL of soluble fraction was collected and stored on ice until use. Similarly, a soluble protein fraction was prepared from an *M. smegmatis* mc^{2}155 cell culture. The soluble protein fraction from induced *E. coli* (pSAU1049) cells was also made using the method of Ganguly et al. (*10*). After estimation of the protein content in each fraction by the method of Bradford (*24*), aliquots from all protein fractions were analyzed by SDS−13.5% PAGE along with known amounts of His-CI. Separated protein bands were transferred to a nitrocellulose membrane followed by the treatment of the membrane sequentially with a 3% BSA, rabbit anti-CI antibody, goat anti-rabbit antibody IgG1-AP (Santa Cruz Biotechnology), and NBT-BCIP (Bangalore Genei) solution for 1−2 h at room temperature. Each incubation step was followed by an adequate washing step. The intensity of each CI-specific band was determined by densitometric scanning of the developed membrane and used in calculating the CI concentration in L1 lysogens.

RESULTS AND DISCUSSION

Bases, Strands, and Grooves of the O_{64} DNA Helix Interacting with L1 CI. Previously, DNase I footprinting analysis demonstrated that the phage L5 repressor interacts with ~25 bp of an L5 DNA fragment harboring a 13 bp asymmetric operator (5′-GGTGGCTGTCAAG-3′) (*20*). We also reported that L1 CI binds efficiently to 21 bp synthetic DNAs carrying the operator sequence mentioned above (*10*). To determine whether CI indeed binds to the 13 bp operator DNA, we have performed the G base-specific DMS protection assay in the presence or absence of a saturating amount of His-CI and ^{32}P-labeled O_{64} DNA. As shown in Figure 1A, the intensities of four top strand G bases and one bottom strand G base of O_{64} DNA are decreased significantly in the presence of His-CI. These His-CI-protected guanine bases correspond to 22G, 23G, 25G, and 29G (all in the top strand) and 31′G (in the bottom strand) (Figure 1D). All the protected G bases are located in the 13 bp operator region, confirming the interaction between CI and asymmetric operator DNA. Notably, the intensities of some top strand G bases (4G, 8G, 18G, and 38G) are also increased in the presence of His-CI. These bases possibly became more exposed due to the conformational change of operator DNA upon His-CI binding.

The N7 group of the guanine base, one of the targets of DMS-mediated methylation, is exposed in the major groove of the DNA helix (*2*), further indicating that the interaction between the CI and operator DNA may occur through this groove of the operator DNA. Helical representation indeed suggests that 22G, 23G, 25G, and 31′G (all encircled, Figure 1E) are distributed in the two adjacent major grooves of O_{64} operator DNA. These bases possibly contact CI from the front of the helix. Contrary to what was described above, 29G (squared) may contact CI from the back of the helix. The way the NTD contacts 29G is not clear at present.

To understand the CI−O_{64} DNA interaction in depth, we also performed a hydroxyl radical footprinting experiment in the presence or absence of a saturating amount of His-CI and ^{32}P-labeled O_{64} DNA (see Experimental Procedures for details). Panels B and C of Figure 1 show the autoradiographs and the corresponding densitometric traces of the hydroxyl radical

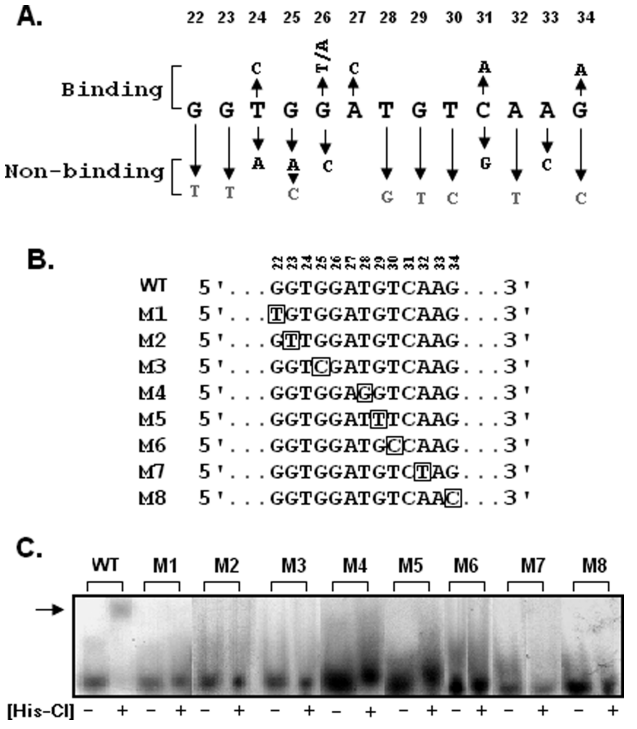

FIGURE 2: Effects of operator DNA mutations on CI binding. (A) Operator DNA bases interacting with repressor. The data reported previously by Hatfull and colleagues (*20*) and our results presented in panel C (see below) are summarized here. Bases (larger font) in one strand of 13 bp O_{64} DNA are shown and numbered 22−34 (to be consistent with the results presented in Figure 1). Naturally occurring base changes (smaller font) in the operator region that affect binding (Nonbinding) or do not affect binding (Binding) of CI are shown. Mutated bases (gray) in the synthesized operators (see panel B) are shown. (B) Synthetic DNA fragments harboring wild-type (WT) or mutated O_{64} operators (M1 to M8). For the sake of simplicity, 13 bases of only one strand are shown and numbered as in panel A. Mutated bases in the operator regions are boxed. (C) Autoradiogram of the gel shift assay performed with (+) and without (−) His-CI and the labeled DNA fragments mentioned in panel B. The arrow denotes the His-CI−operator complex.

footprints, respectively. The data demonstrate that top and bottom strands of O_{64} DNA harbor three (a, b, and c) and two (a′ and b′) His-CI-protected regions, respectively. The protected regions are 4−5 bp long and cover nearly 20 bp encompassing the 13 bp operator sequence (Figure 1C). While regions b and b′ are strongly protected, regions a and a′ are moderately protected, and region c is weakly protected under the conditions of the experiment. The interaction between CI and O_{64} DNA is, therefore, asymmetric in nature. The data also suggest that an additional 3 bp at both sides of the 13 bp O_{64} DNA might be critical for repressor binding. Moreover, the centers of two adjacent protected regions are 9−10 bp long, indicating that one face of O_{64} DNA helix might be involved in the interaction with CI (Figure 1D).

Operator Mutations Affecting the Binding of L1 CI. Our DMS footprinting study (see above) reveals that five guanine bases, distributed in the top and bottom strands of 13 bp O_{64} DNA, are critical for repressor recognition. Previous in vitro studies showed that the L5 repressor (*20*) does not bind to the operator DNA with a G25A or C31G change (Figure 2A). Additionally, operator DNAs with T24A, G26C, and A33C substitutions did not interact with L5 repressor. Interestingly, operator DNAs with T24C, G26T/A, A27C, C31A, and G34A substitutions showed binding with L5 repressor, indicating that

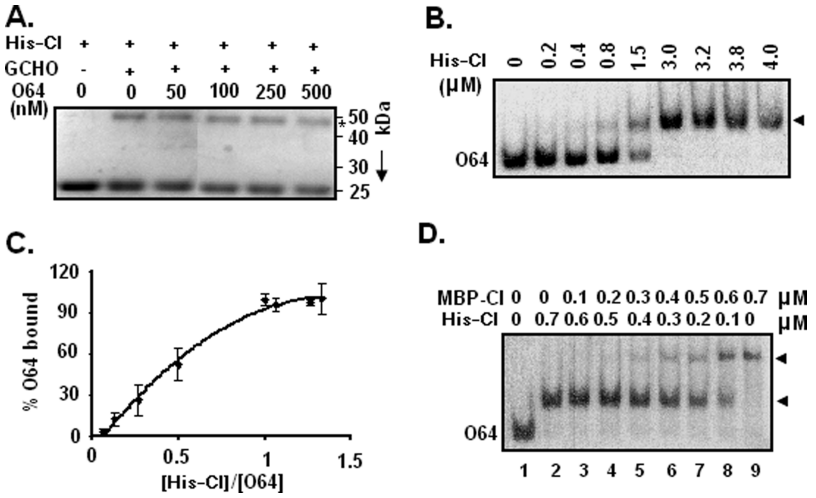

FIGURE 3: Binding stoichiometry. (A) SDS−PAGE analysis of glutaraldehyde (GCHO)-treated His-CI. Reaction mixtures containing a fixed amount of His-CI and the indicated amounts of O_{64} DNA were treated with (+) or without (−) 0.1% GCHO. Masses (kilodaltons) of marker protein bands are shown at the right side of the gel. The asterisk denotes dimeric His-CI. (B) Gel shift assay with excess O_{64} DNA. The autoradiogram shows the interaction between the indicated amounts of His-CI and the stoichiometric amount of O_{64} DNA (see Experimental Procedures for details). The arrowhead indicates the His-CI−O_{64} DNA complex. (C) Plot of percent O_{64} DNA bound vs [His-CI]/[O_{64} DNA]. The fractions of O_{64} DNA bound by His-CI (in percent) were determined as described in Experimental Procedures. The error bars indicate standard deviations of three independent experiments. (D) Mixed oligomerization assay. The assay was performed as described in Experimental Procedures. The autoradiogram demonstrates the binding of the ^{32}P-labeled O_{64} DNA with the indicated amounts of His-CI (lane 2), MBP-CI (lane 9), and His-CI with MBP-CI (lanes 3−8). Lane 1 contained free O_{64} DNA. The arrowhead indicates MBP-CI or His-CI−O_{64} DNA complexes.

the base pair changes at positions 24, 26, 27, 31, and 34 are partly tolerable. To confirm whether bases at positions 22, 23, 25, 28−30, 32, and 33 in the 13 bp operator DNA are absolutely critical for repressor binding, we performed gel shift assays using different mutant operator DNAs [namely, M1−M8 (Figure 2B)] and His-CI and compared the results with that performed in the presence of wild-type O_{64} DNA. As evident from Figure 2C, mutant operator DNAs with G22T, G23T, G25C, T28G, G29T, T30C, A32T, and G34C substitutions did not show detectable binding by His-CI (even after long exposure), indicating that the base alternations described above are not tolerable for repressor binding. The exact base pair specificity of L1 repressor in all but one position of the 13 bp operator DNA is not known; however, we noticed that eight of 13 repressor interacting bases are located in the two adjacent major grooves of operator DNA (Figure 1D).

Binding Stoichiometry. The CI concentrations that yielded half-maximal binding of different L1 operator DNAs (i.e., K_d values) range from ~140 to ~370 nM (*10*). In contrast, the K_d values for His-CI−O_{64} DNA and MBP-CI−O_{64} DNA interactions are ~250 (*19*) and ~315 nM, respectively (Figure S1B of the Supporting Information). At ~200 nM, CI was shown to exist as a mixture of monomers and dimers in solution (*10*), suggesting that CI, like λ repressor (*2*), possibly binds to the cognate operator DNA as a dimer. Interaction of His-CI with two adjacent major grooves in the helical O_{64} DNA [as evident from our footprinting analyses (see above)] tends to agree with the hypothesis mentioned above. However, equilibrium binding data of L1 repressor suggested that CI binds to the cognate operator DNA as a monomer (*10*). To resolve the contradiction about the repressor binding stoichiometry, we performed the glutaraldehyde-mediated cross-linking of His-CI in the presence of varying concentrations of O_{64} DNA (Figure 3A). On the basis of results with other repressor proteins (*29*, *30*), dimerization of His-CI would be induced by O_{64} DNA if the operator binding form of this repressor is dimeric in nature. The intensity of dimeric His-CI (~50 kDa), however, remained nearly unaltered when His-CI was incubated with O_{64} DNA prior to cross-linking, suggesting that binding to O_{64} DNA does not involve the dimerization of His-CI under the conditions used here.

As the chemical cross-linking experiment is relatively insensitive, we conducted a gel shift assay using larger amounts of both His-CI and O_{64} DNA. The concentration of operator DNA in this assay was kept fixed nearly 12-fold above K_d to strongly promote repressor binding. Under the stoichiometric conditions mentioned above, almost all the operator DNA was shifted in the presence of 3−4 μM His-CI (Figure 3B). The plot of binding of His-CI to O_{64} DNA, generated using the data from three independent gel shift assays, demonstrates that His-CI binding reaches saturation when the ratio of His-CI to O_{64} DNA concentrations is ≳1 (Figure 3C). Under similar experimental conditions, many repressor proteins that bind to their cognate operator DNAs as dimers (*2*, *30*, *31*) show binding saturation at a repressor to operator ratio of 2. Gel shift assay results, therefore, support the chemical cross-linking data, and they together suggest that the apparent binding stoichiometry is one CI monomer per O_{64} DNA.

To confirm the results described above, we performed the mixed oligomerization assay using end-labeled O_{64} DNA and MBP-CI and/or His-CI (see Experimental Procedures). The MBP-CI repressor carries 355 amino acid residues more at its N-terminal end than does His-CI. As a result, the shifted band (lane 9) formed by MBP-CI and O_{64} DNA exhibited a relatively slower migration than the shifted band (lane 2) generated with His-CI and O_{64} DNA (Figure 3D). In contrast, two types of shifted bands appeared when different (pre-equilibrated) mixtures of MBP-CI and His-CI were incubated with O_{64} DNA (lanes 3−8). Apparently, migrations of the bands mentioned above resemble those of the shifted bands formed either by MBP-CI and O_{64} DNA alone or by His-CI and O_{64} DNA alone. If a repressor binds to the asymmetric operator DNA as a dimer or higher oligomer, more than two shifted bands would appear in the presence of both MBP-CI and His-CI. The additional band(s)

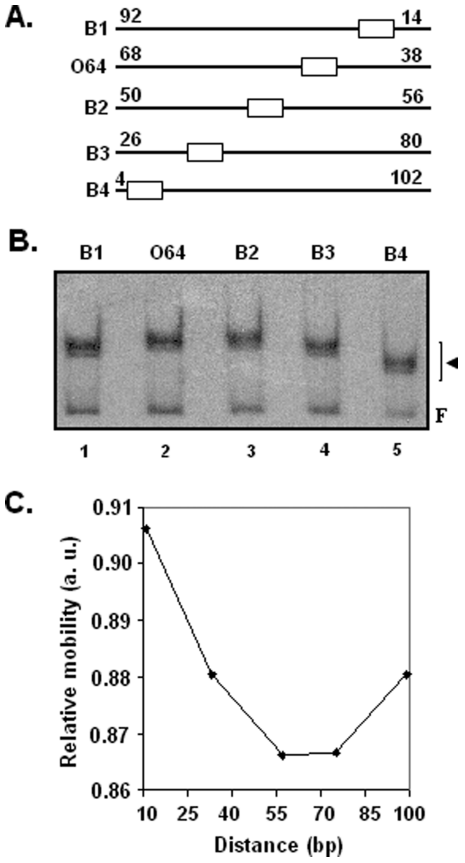

FIGURE 4: DNA bending study. (A) DNA fragments for the bending experiment. All DNA fragments were PCR amplified using specific primer pairs and p1223 DNA (see Experimental Procedures and Table 1 for details). White rectangles in the DNA fragments denote 13 bp O_{64} DNA. Distances (in base pairs) of the 13 bp O_{64} DNA from either the 5′ or 3′ end are shown. (B) Gel shift assay. The autoradiogram shows the binding between different ^{32}P-labeled DNA fragments and His-CI. Lanes 1−5 contained His-CI−operator complexes (indicated by the arrowhead) formed with the B1, O64, and B2−B4 DNAs, respectively. F indicates free DNA. (C) Mobilities of the His-CI−DNA complexes determined from the autoradiogram (see Experimental Procedures for details) and plotted vs the distances (in base pairs) of the 13 bp O_{64} operator in the DNA fragments mentioned above.

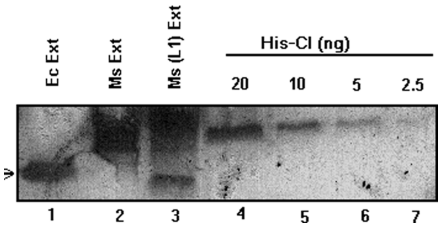

FIGURE 5: Intracellular CI concentration. The CI level in the L1 lysogen was determined by Western analysis of different crude extracts and indicated amounts of His-CI according to a standard method (see Experimental Procedures for details). Ms Ext, Ms (L1) Ext, and Ec Ext denote crude extracts from *M. smegmatis* mc^{2}155, L1 lysogen, and *E. coli* (pSAU1049) cells, respectively. The arrow indicates CI.

could have arisen by binding of the hybrid repressor dimers [formed due to the random assortment between the MBP-CI and His-CI monomers (Figure S1C)] to O_{64} DNA. Surprisingly, we did not detect any additional band between the MBP-CI- and His-CI-generated bands [even after long exposure of the film (data not shown)], indicating that the species binding to O_{64} operator DNA is a repressor monomer.

Bending of O_{64} DNA. In numerous instances, operator DNA bending induced by many phage repressors (*32*−*34*) has been demonstrated to be critical for phage-specific gene expression. Our DMS protection experiment (see above) also hints at possible L1 repressor-mediated bending of O_{64} DNA. To determine whether CI truly induces bending in the cognate operator DNA, we performed a gel shift assay using His-CI and five DNA fragments (119 bp each) carrying 13 bp O_{64} DNA at different locations (Figure 4A). Figure 4B shows that DNA fragments bound to the repressor migrated differently despite their identical lengths (lanes 1−5). In contrast, migrations of free DNAs are nearly identical, indicating that the sequences of these DNAs produced very little intrinsic curvature. Maximum retardation was observed with B2 DNA that harbors O_{64} approximately at the middle of the fragment. An apparent bending angle, determined using the normalized shifts from three independent experiments, was 30 ± 3.63°, suggesting that CI does cause bending of O_{64} DNA. In addition, the apparent bending center was found within the O_{64} DNA (Figure 4C). The CI-induced bending noted above is relatively weak in comparison with the bending observed with various other phage-specific repressors (*32*−*34*). The λ phage-specific Int, a protein involved in site-specific homologous recombination, however, feebly induces bending in the cognate P1 site (*35*). The weak CI-induced bending of O_{64} DNA, therefore, could be regulating the L1 gene expression by a mechanism that is not clear at present.

In Vivo Concentration of L1 Repressor. L5 harbors 30 homologous CI-binding operator sites at various genome locations (*9*, *20*). Being a minor variant of L5 (*16*, *18*), the L1 genome might also be composed of multiple operator sites, including O_{64} and O_L. If the hypothesis given above is true, a relatively high level of CI needs to be synthesized for all these operator sites in an L1 lysogen to be shut off. To see whether the intracellular CI level is indeed very high, we performed Western blotting experiments using the polyclonal anti-CI antibody, soluble protein extracts from an L1 lysogen, *M. smegmatis* and *E. coli* expressing CI, and varying amounts (2.5−20 *n*g) of His-CI (see Experimental Procedures for details). As demonstrated in Figure 5, a protein band was found in the soluble fraction of the L1 lysogen (lane 3) that was absent in the *M. smegmatis* extract (lane 2). This protein seems to be CI as its molecular mass matches that of CI (lane 1). The anti-CI antibody also recognized His-CI (lanes 4−7) as expected. Intensities of all repressor-specific protein bands were determined by densitometric scanning. The plot of the intensity of repressor-specific protein bands versus the amount of His-CI (data not shown), which was generated using the scanned data from two independent Western blot experiments, indicates that the amount of CI is ~2.9 ± 0.2 μg in 6 × 10^{10} mc^{2}155 (L1) cells used for making the protein extract. Considering a molecular mass of 22000 Da for a CI monomer, each L1 lysogen was calculated to possess nearly 1319 ± 83 repressor monomers for 30 operators (i.e., 44 ± 2.8 repressor monomers for repressing each operator). Interestingly, a λ lysogen was also reported to synthesize ~42 repressor monomers for each of six λ operator DNAs (*36*).

The biological significance of the elevated level of the repressor in an L1 lysogen is not known with certainty. Apart from ensuring complete repression of the 30 operator DNAs, it may influence dimerization of the repressor in an L1 lysogen. Repressor dimers, once generated, may be used to regulate L1 gene expression by binding to the asymmetric operator DNAs.

Our previous gel filtration experiment (*10*) and the footprinting studies conducted here (Figure 1) both support the hypothesis given above; however, studies of the binding stoichiometry (Figure 3) have contradicted it. The L1 repressor−operator DNA complex, therefore, seems to attain a tertiary structure that is distinct from those formed between the dimeric repressors and cognate operator DNAs of the lambdoid phages (*2*). To the best of our knowledge, the only repressor that exhibited a footprinting pattern similar to that of the L1 repressor is synthesized by temperate *Bacillus subtilis* phage Φ105 (*7*). Incidentally, Φ105 repressor also binds to an asymmetric operator DNA, but its binding stoichiometry and intracellular level have not been determined. The binding stoichiometry exhibited by the L1 repressor, though not reported for any other repressor, is, however, not unique. Several eukaryotic transcription factors like NFAT (*37*), GATA-1 (*38*), and TTF-1 (*39*), and the T4 phage-specific transcription factor, MotA (*40*), have shown binding to their respective DNAs as monomers.

CONCLUSIONS

This investigation has provided valuable insights into the tertiary structure of the L1 repressor−asymmetric operator complex. In addition to several bases, two adjacent major grooves on one face of the asymmetric operator DNA helix are crucial for repressor binding. Unexpectedly, L1 repressor that induces weak bending in the operator DNA exhibited binding as a monomer even though the concentration of L1 repressor per operator was found to be nearly the same as that of the λ phage system. The architecture of the L1 repressor−operator complex, therefore, seems to be structurally distinct from those of the lambdoid phages.

ACKNOWLEDGMENT

We are extremely grateful to Drs. N. C. Mandal (Ex-Emeritus Professor, Bose Institute), K. Sau (Haldia Institute of Technology, Haldia, India), G. Chakrabarti (University of Calcutta, Calcutta, India), and D. Cue (University of Arkansas for Medical Sciences, Little Rock, AR) for their valuable suggestions during the work and for critically reading and rectifying the manuscript. We also thank Mr. A. Banerjee, Mr. A. Poddar, Mr. J. Guin, and Mr. M. Das for their excellent technical support.

SUPPORTING INFORMATION AVAILABLE

Supplemental figure. This material is available free of charge via the Internet at http://pubs.acs.org.

REFERENCES

1. Winston, F., and Botstein, D. (1981) Control of lysogenization by phage P22. I. The P22 *cro* gene. *J. Mol. Biol. 152*, 209–232.
2. Gussin, G. N., Johnson, A. D., Pabo, C. O., and Sauer, R. T. (1983) in Repressor and Cro Protein: Structure, Function, and Role in Lysogenization. Lambda II (Hendrix, R. W., Roberts, J. W., Stahl, F. W., and Weisberg, R. A., Eds.) pp 93− 121, Cold Spring Harbor Laboratory Press, Plainview, NY.
3. Ogawa, T., and Ogawa, H. (1988) Organization of the early region of bacteriophage 80. *J. Mol. Biol. 202*, 537–550.
4. Oberto, J., Weisberg, R. A., and Gottesman, M. E. (1989) Structure and function of the *nun* gene and the immunity region of the lambdoid phage HK022. *J. Mol. Biol. 207*, 675–693.
5. Rousseau, P., Betermier, M., Chandler, M., and Alazard, R. (1996) Interactions between the repressor and the early operator region of bacteriophage Mu. *J. Biol. Chem. 271*, 9739–9745.
6. Koudelka, A. P., Hufnagel, L. A., and Koudelka, G. B. (2004) Purification and characterization of the repressor of the shiga toxin-encoding bacteriophage 933W: DNA binding, gene regulation, and autocleavage. *J. Bacteriol. 186*, 7659–7669.
7. van Kaer, L., van Montagu, M., and Dhaese, P. (1989) Purification and *in vitro* DNA-binding specificity of the *Bacillus subtilis* phage φ105 repressor. *J. Biol. Chem. 264*, 14784–14791.
8. Heinrich, J., Velleman, M., and Schuster, H. (1995) The tripartite immunity system of phages P1 and P7. *FEMS Microbiol. Rev. 1995* (17), 121–126.
9. Hatfull, G. F. (2000) Molecular Genetics of Mycobacteria, ASM Press, Washington, DC.
10. Ganguly, T., Bandhu, A., Chattoraj, P., Chanda, P. K., Das, M., Mandal, N. C., and Sau, S. (2007) Repressor of temperate mycobacteriophage L1 harbors a stable C-terminal domain and binds to different asymmetric operator DNAs with variable affinity. *Virol. J. 4*, 64.
11. Koudelka, G. B., Harrison, S. C., and Ptashne, M. (1987) Effect of non-contacted bases on the affinity of 434 operator for 434 repressor and Cro. *Nature 326*, 886–888.
12. Knight, K. L., and Sauer, R. T. (1992) Biochemical and genetic analysis of operator contacts made by residues within the β-sheet DNA binding motif of Mnt repressor. *EMBO J. 11*, 215–223.
13. Nelson, H. C. M., and Sauer, R. T. (1985) Lambda repressor mutations that increase the affinity and specificity of operator binding. *Cell 42*, 549–558.
14. Snapper, S. B., Lugosi, L., Jekkel, A., Melton, R. E., Kieser, T., Bloom, B. R., and Jacobs, W. R., Jr. (1988) Lysogeny and transformation in mycobacteria: Stable expression of foreign genes. *Proc. Natl. Acad. Sci. U.S.A. 85*, 6987–6991.
15. Chaudhuri, B., Sau, S., Datta, H. J., and Mandal, N. C. (1993) Isolation, characterization, and mapping of temperature-sensitive mutations in the genes essential for lysogenic and lytic growth of the mycobacteriophage L1. *Virology 194*, 166–172.
16. Sau, S., Chattoraj, P., Ganguly, T., Lee, C. Y., and Mandal, N. C. (2004) Cloning and sequencing analysis of the repressor gene of temperate mycobacteriophage L1. *J. Biochem. Mol. Biol. 37*, 254–259.
17. Ganguly, T., Chanda, P. K., Bandhu, A., Chattoraj, P., Das, M., and Sau, S. (2006) Effects of physical, ionic, and structural factors on the binding of repressor of mycobacteriophage L1 to its cognate operator DNA. *Protein Pept. Lett. 13*, 793–798.
18. Ganguly, T., Chattoraj, P., Das, M., Chanda, P. K., Mandal, N. C., Lee, C. Y., and Sau, S. (2004) A point mutation at the C-terminal half of the repressor of temperate mycobacteriophage L1 affects its binding to the operator DNA. *J. Biochem. Mol. Biol. 37*, 709–714.
19. Bandhu, A., Ganguly, T., Chanda, P. K., Das, M., Jana, B., Chakrabarti, G., and Sau, S. (2009) Antagonistic effects Na^+ and Mg^{2+} on the structure, function, and stability of mycobacteriophage L1 repressor. *BMB Rep. 42*, 293–298.
20. Brown, K. L., Sarkis, G. J., Wadsworth, C., and Hatfull, G. F. (1997) Transcriptional silencing by the mycobacteriophage L5 repressor. *EMBO J. 16*, 5914–5921.
21. Chattopadhyay, C., Sau, S., and Mandal, N. C. (2003) Cloning and characterization of the promoters of temperate mycobacteriophage L1. *J. Biochem. Mol. Biol. 36*, 586–592.
22. Sambrook, J., and Russell, D. W. (2001) Molecular Cloning: A Laboratory Manual, 3rd ed., Cold Spring Harbor Laboratory Press, Plainview, NY.
23. Ausubel, F. M., Brent, R., Kingston, R. E., Moore, D. D., Seidman, J. G., Smith, J. A., and Struhl, K. (1998) Current Protocols in Molecular Biology, John Wiley & Sons, Inc., New York.
24. Bradford, M. M. (1976) A rapid and sensitive method for the quantitation of microgram quantities of protein utilizing the principle of protein-dye binding. *Anal. Biochem. 72*, 248–254.
25. Chattoraj, P., Ganguly, T., Nandy, R. K., and Sau, S. (2008) Overexpression of a delayed early gene *hlg1* of temperate mycobacteriophage L1 is lethal to both *M. smegmatis* and *E. coli*. *BMB Rep. 41*, 363–368.
26. Ramesh, V., and Nagaraja, V. (1996) Sequence-specific DNA binding of the phage Mu C protein: Footprinting analysis reveals altered DNA conformation upon protein binding. *J. Mol. Biol. 260*, 22–33.
27. Kim, J., Zwieb, C., Wu, C., and Adhya, S. (1989) Bending of DNA by gene-regulatory proteins: Construction and use of a DNA bending vector. *Gene 85*, 15–23.
28. Maxam, A. M., and Gilbert, W. (1980) Sequencing end-labeled DNA with base-specific chemical cleavages. *Methods Enzymol. 65*, 499–560.
29. Kukolj, G., Tolias, P. P., Autexier, C., and DuBow, M. S. (1989) DNA-directed oligomerization of the monomeric Ner repressor from the Mu-like bacteriophage D108. *EMBO J. 8*, 3141–3148.

30. Ganguly, T., Das, M., Bandhu, A., Chanda, P. K., Jana, B., Mondal, R., and Sau, S. (2009) Physicochemical properties and distinct DNA binding capacity of the repressor of temperate *Staphylococcus aureus* phage ϕ11. *FEBS J. 276*, 1975–1985.
31. Hendrickson, W., and Schleif, R. (1985) A dimer of araC protein contacts three adjacent major groove regions of the aria DNA site. *Proc. Natl. Acad. Sci. U.S.A. 82*, 3129–3133.
32. Lyubchenko, Y., Shlyakhtenko, L., Chernov, B., and Harrington, R. E. (1991) DNA bending induced by Cro protein binding as demonstrated by gel electrophoresis. *Proc. Natl. Acad. Sci. U.S.A. 88*, 5331–5334.
33. Koudelka, G. B. (1991) Bending of synthetic bacteriophage 434 operators by bacteriophage 434 proteins. *Nucleic Acids Res. 19*, 4115–4119.
34. Ahlgren-Berg, A., Henriksson-Peltola, P., Sehlén, W., and Haggard-Ljungquist, E. (2007) A comparison of the DNA binding and bending capacities and the oligomeric states of the immunity repressors of heteroimmune coliphages P2 and WΦ. *Nucleic Acids Res. 35*, 3167–3180.
35. Thompson, J. F., and Landy, A. (1988) Empirical estimation of protein-induced DNA bending angels: Applications to λ site-specific recombination complexes. *Nucleic Acids Res. 16*, 9687–9705.
36. Oppenheim, A. B., Kobiler, Stavans, O. J., Court, D. L., and Adhya, S. (2005) Switches in bacteriophage λ development. *Annu. Rev. Genet. 39*, 409–429.
37. Stroud, J. C., and Chen, L. (2003) Structure of NFAT bound to DNA as monomer. *J. Mol. Biol. 334*, 1009–1022.
38. Omichinski, J. G., Trainor, C., Evans, T., Gronenborn, A. M., Clore, G. M., and Felsenfeld, G. (1993) A small single-"finger" peptide from the erythroid transcription factor GATA-1 binds specifically to DNA as a zinc or iron complex. *Proc. Natl. Acad. Sci. U.S.A. 90*, 1676–1680.
39. Damante, G., Tell, G., Leonardi, A., Fogolari, F., Bortolotti, N., Di Lauro, R., and Formisano, S. (1994) Analysis of the conformation and stability of rat TTF-1 homeodomain by circular dichroism. *FEBS Lett. 354*, 293–296.
40. Cicero, M. P., Alexander, K. A., and Kreuzer, K. N. (1998) The MotA transcriptional activator of bacteriophage T4 binds to its specific DNA site as a monomer. *Biochemistry 37*, 4977–4984.